

Negative impact of heavy-tailed uncertainty and error distributions on the reliability of calibration statistics for machine learning regression tasks

Pascal PERNOT ¹

*Institut de Chimie Physique, UMR8000 CNRS,
Université Paris-Saclay, 91405 Orsay, France^{a)}*

Average calibration of the (variance-based) prediction uncertainties of machine learning regression tasks can be tested in two ways: one is to estimate the calibration error (CE) as the difference between the mean absolute error (MSE) and the mean variance (MV); the alternative is to compare the mean squared z -scores (ZMS) to 1. The problem is that both approaches might lead to different conclusions, as illustrated in this study for an ensemble of datasets from the recent machine learning uncertainty quantification (ML-UQ) literature. It is shown that the estimation of MV, MSE and their confidence intervals becomes unreliable for heavy-tailed uncertainty and error distributions, which seems to be a frequent feature of ML-UQ datasets. By contrast, the ZMS statistic is less sensitive and offers the most reliable approach in this context, still acknowledging that datasets with heavy-tailed z -scores distributions should be considered with great care. Unfortunately, the same problem is expected to affect also *conditional* calibrations statistics, such as the popular ENCE, and very likely *post-hoc* calibration methods based on similar statistics. Several solutions to circumvent the outlined problems are proposed.

This preprint is a revised and extended version of “How to validate average calibration for machine learning regression tasks?” (<https://arxiv.org/abs/2402.10043v2>).

^{a)}Electronic mail: pascal.pernot@cnrs.fr

I. INTRODUCTION

The assessment of prediction uncertainty calibration for machine learning (ML) regression tasks is based on two main types of statistics: (1) the calibration errors (RCE, UCE, ENCE...) ^{1,2} which are based on the comparison of the mean squared errors (MSE) to mean squared uncertainties or mean variance (MV); and (2) the Negative Log-Likelihood (NLL) ³⁻⁵ which is based on the mean of squared z-scores or scaled errors (ZMS) ². The comparison of MSE to MV has been used to test or establish *average* calibration ^{6,7}, but it mostly occurs in ML through a bin-based setup ¹, meaning that it measures local or *conditional* calibration.

Average calibration is known to be insufficient to guarantee the reliability of uncertainties across data space ⁸, but it remains a necessary condition that is too often overlooked in calibration studies. Moreover, an interest of the RCE and ZMS statistics is to have predefined reference values, enabling direct statistical testing of average calibration. This is not the case for bin-based statistics such as the UCE and ENCE, for which validation is much more complex ⁹. *De facto*, the latter are practically used only in comparative studies, without validation.

This study focuses on the comparison of RCE- and ZMS-based approaches to validate calibration, and is motivated by the observation that both approaches might lead to conflicting diagnostics when applied to ML uncertainty quantification (ML-UQ) datasets. Understanding the origin of such discrepancies is important to assess the reliability of these calibration statistics and their bin-based extensions.

The next section defines the calibration statistics and the validation approach. Sect. III introduces the ML-UQ datasets used to illustrate the validation results, with a focus on the shape of their uncertainty and error distributions. Numerical experiments, based on synthetic datasets mimicking the real datasets, are performed in Sect. IV, in order establish the impact of the tailedness of the uncertainty and error distributions on the reliability of the calibration statistics. Sect. V illustrates this reliability issue on the reference ML-UQ datasets for RCE and ZMS. The conclusions are presented in Sect. VI, along with a proposition of solutions.

Note: A compilation of 33 datasets of ML materials properties published after the completion of this study has been included *a posteriori* in Sect. VD to assess the general validity of the main observations.

II. AVERAGE CALIBRATION STATISTICS

Let us consider a dataset composed of *paired* errors and uncertainties $\{E_i, u_{E_i}\}_{i=1}^M$ to be tested for *average* calibration. The variance-based UQ validation statistics are built on a probabilistic model linking errors to uncertainties

$$E_i \sim u_{E_i} D(0, 1) \quad (1)$$

where $D(\mu, \sigma)$ is an unspecified probability density function with mean μ and standard deviation σ . This model states that errors are expected to be unbiased ($\mu = 0$) and that uncertainty quantifies the *dispersion* of errors, according to the metrological definition¹⁰.

A. The calibration error and related statistics

Let us assume that the errors are drawn from a distribution $D(0, \sigma)$ with an unknown scale parameter σ , itself distributed according to a distribution G . The distribution of errors is then a *scale mixture distribution* H , with probability density function

$$p_H(E) = \int_0^\infty p_D(E|\sigma) p_G(\sigma) d\sigma \quad (2)$$

and the variance of the compound distribution of errors is obtained by the *law of total variance*

$$\text{Var}(E) = \langle \text{Var}_D(E|\sigma) \rangle_G + \text{Var}_G(\langle E|\sigma \rangle_D) \quad (3)$$

$$= \langle u_E^2 \rangle + \text{Var}_G(\langle E|\sigma \rangle_D) \quad (4)$$

where the first term of the RHS of Eq. 3 has been identified as the mean squared uncertainty $\langle u_E^2 \rangle$. This expression can be compared to the standard expression for the variance

$$\text{Var}(E) = \langle E^2 \rangle - \langle E \rangle^2 \quad (5)$$

For an unbiased error distribution, one gets $\text{Var}_G(\langle E|\sigma \rangle_D) = 0$ and $\langle E \rangle = 0$, leading to

$$\langle E^2 \rangle = \langle u_E^2 \rangle \quad (6)$$

Based on this equation, the Relative Calibration Error, aimed to test average calibration, is defined as

$$RCE = \frac{RMV - RMSE}{RMV} \quad (7)$$

where $RMSE$ is the root mean squared error $\sqrt{\langle E^2 \rangle}$ and RMV is the root mean variance ($\sqrt{\langle u_E^2 \rangle}$). The reference value to validate the RCE is 0.

The RCE is rarely used as such, but it occurs in a bin-based statistic of *conditional calibration*,² the Expected Normalized Calibration Error¹

$$ENCE = \frac{1}{N} \sum_{i=1}^N |RCE_i| \quad (8)$$

where RCE_i is estimated over the data in bin i . Depending on the variable chosen to design the bins, the ENCE might be used to test *consistency* (binning on u_E) or *adaptivity* (binning on input features)². The ENCE has no predefined reference value (it depends on the dataset and the binning scheme)⁹, which complicates the statistical testing of conditional calibration.

B. ZMS and related statistics

Another approach to calibration based on Eq. 1 uses z-scores

$$Z_i = \frac{E_i}{u_{E_i}} \sim D(0, 1) \quad (9)$$

with the property

$$Var(Z) = 1 \quad (10)$$

assessing average calibration for unbiased errors^{11,12}. If one accepts that the uncertainties have been tailored to cover biased errors, the calibration equation becomes

$$ZMS = \langle Z^2 \rangle = 1 \quad (11)$$

which is the preferred form for testing², notably when a dataset is split into subsets for the assessment of conditional calibration. The target value for statistical validation of the ZMS is 1.

The negative log-likelihood (NLL) score for a normal likelihood is linked to the ZMS by¹³

$$NLL = \frac{1}{2} \left(\langle Z^2 \rangle + \langle \ln u_E^2 \rangle + \ln 2\pi \right) \quad (12)$$

It combines the ZMS as an *average calibration* term¹⁴ to a *sharpness* term driving the uncertainties towards small values¹⁵ when the NLL is used as a loss function, hence preventing the minimization of $\langle Z^2 \rangle$ by arbitrary large uncertainties. For a given set of uncertainties, testing the NLL value is equivalent to testing the ZMS value.

As for the RCE, the ZMS can be used to validate conditional calibration through a bin-based approach, the Local ZMS (LZMS) analysis².

C. Validation

Considering that errors and uncertainties have generally non-normal distributions, and that it is not reliable to invoke the Central Limit Theorem to use normality-based testing approaches (see Pernot¹¹), one has to infer confidence intervals on the statistics by bootstrapping (BS) for comparison to their reference values.

For a given dataset (E, u_E) and a statistic ϑ , one estimates the statistic over the dataset, ϑ_{est} , and a bootstrapped sample from which one gets the bias of the bootstrapped distribution b_{BS} and a 95% confidence interval $I_{BS} = [I_{BS}^-, I_{BS}^+]$. Note that it is generally not recommended to correct ϑ_{est} from the bootstrapping bias b_{BS} , but it is important to check that the bias is negligible. One of the most reliable BS approaches in these conditions is considered to be the Bias Corrected Accelerated (BC_a) method¹⁶, which is used throughout this study.

Validation is then done by checking that the target value for the statistic, ϑ_{ref} , lies within I_{BS} , i.e.

$$\vartheta_{ref} \in [I_{BS}^-, I_{BS}^+] \quad (13)$$

To go beyond this binary result, it is interesting to have a continuous measure of agreement, and one can define a standardized score ζ as the ratio of the signed distance of the estimated value ϑ_{est} to its reference ϑ_{ref} , over the absolute value of the distance between ϑ_{est} and the limit of the confidence interval closest to ϑ_{ref} . More concretely

$$\zeta(\vartheta_{est}, \vartheta_{ref}, I_{BS}) = \begin{cases} \frac{\vartheta_{est} - \vartheta_{ref}}{I_{BS}^+ - \vartheta_{est}} & \text{if } (\vartheta_{est} - \vartheta_{ref}) \leq 0 \\ \frac{\vartheta_{est} - \vartheta_{ref}}{\vartheta_{est} - I_{BS}^-} & \text{if } (\vartheta_{est} - \vartheta_{ref}) > 0 \end{cases} \quad (14)$$

which considers explicitly the asymmetry of I_{BS} around ϑ_{est} . The compatibility of the statistic with its reference value can then be tested by

$$|\zeta(\vartheta_{est}, \vartheta_{ref}, I_{BS})| \leq 1 \quad (15)$$

which is strictly equivalent to the interval test (Eq. 13). In addition to testing, ζ -scores provide valuable information about the sign and amplitude of the mismatch between the statistic and its reference value.

III. ML-UQ DATASETS

Nine test sets, including errors and *calibrated* uncertainties, have been collected from the recent ML-UQ literature for the prediction of various physico-chemical properties by a di-

Set #	Name	Size M	Shape parameter ν		
			u_E^2	E^2	Z^2
1	Diffusion_RF ¹⁸	2040	1.72	2.17	7.91
2	Perovskite_RF ¹⁸	3834	0.79	1.18	4.91
3	Diffusion_LR ¹⁸	2040	5.34	6.32	15.10
4	Perovskite_LR ¹⁸	3836	1.53	2.72	8.15
5	Diffusion_GPR_Bayesian ¹⁸	2040	30.8	2.75	2.72
6	Perovskite_GPR_Bayesian ¹⁸	3818	1.19	0.78	0.85
7	QM9_E ¹⁹	13885	1.91	2.43	3.95
8	logP_10k_a_LS-GCN ⁵	5000	24.7	4.24	3.66
9	logP_150k_LS-GCN ⁵	5000	17.3	10.0	20.2

Table I. The nine datasets used in this study: number, name with reference, size, and shape parameters for the fits of u_E^2 by an Inverse Gamma distribution, and of the E^2 and Z^2 by an F distribution.

verse panel of ML methods. This selection ignored small datasets and those presenting identical properties. Note that for all these datasets, the uncertainties have been calibrated by a palette of methods with various levels of success^{2,17}. The datasets names, sizes, bibliographic references and shape statistics are gathered in Table I, and the reader is referred to the original articles for further details. In the following, a short notation is used, e.g. ‘Set 7’ corresponds to the QM9_E dataset.

As the shape of the distributions of u_E^2 , E^2 and Z^2 is central to the elucidation of the problem presented in the following sections, these were characterized for each dataset as explained below and reported in Table I.

A. u_E^2 distributions

The Inverse-Gamma (IG) distribution²⁰ is commonly used to describe variance (u_E^2) samples

$$u_E^2 \sim \Gamma^{-1}(\alpha = \nu, \beta = \sigma\nu) \quad (16)$$

where $\alpha > 0$ and $\beta > 0$ are the shape and scale parameters, respectively, expressed here as combinations of a number of degrees of freedom ν and a scale factor σ . This equation is more conveniently expressed as

$$u_E^2/\sigma^2 \sim \Gamma^{-1}(\nu, \nu) \quad (17)$$

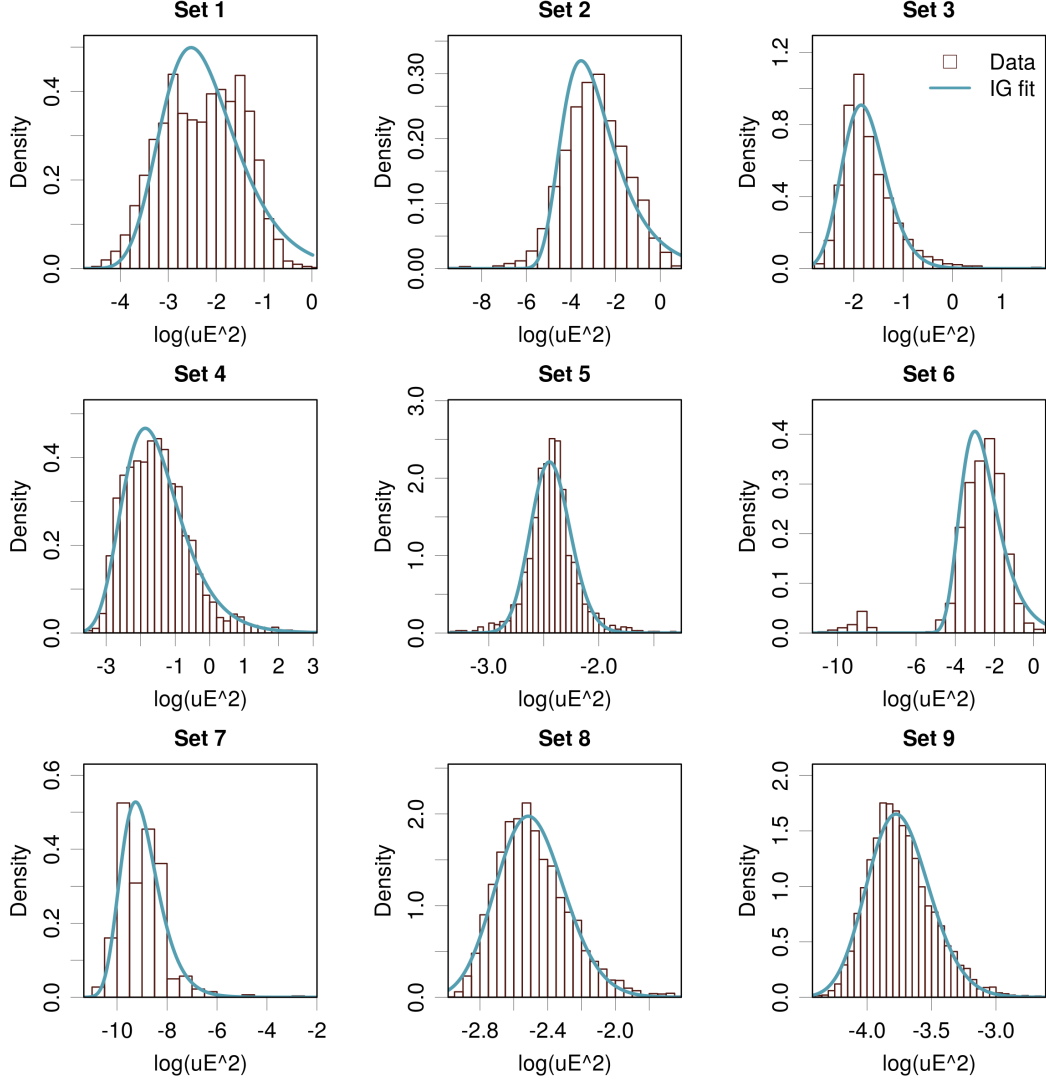


Figure 1. Fit of the squared uncertainties (histogram) by an Inverse-Gamma $\Gamma^{-1}(\nu, \nu)$ distribution (blue line).

This distributions is often used in Bayesian inference as a prior for variance parameters.

Fit of squared uncertainty distributions by the IG model is done by maximum goodness-of-fit estimation using the Kolmogorov-Smirnov distance²¹. The results are shown in Fig. 1, and the shape parameters are reported in Table I.

Overall, the fits are of contrasted quality. The distributions for Sets 1, 2 and 6 are the worst ones, mostly due to the presence of a bimodality (a tiny one for Set 2). The ν values for these sets are very low: for Set 2 $\nu < 1$ corresponds to an IG distributions with undefined mean value, whereas for Sets 1 and 6 values of $\nu < 2$ indicate an undefined variance. These values should not be over-interpreted. Nevertheless, better fitted distributions present also very small shape parameters ($\nu < 2$), such as Sets 4 and 7, meaning that such values might not be unreasonable.

One can thus characterize the variance datasets by their shape parameter ν , which covers a wide range from 0.8 to 31 (Table I).

B. E^2 distributions

Using the generative model, Eq. 1, with a standard normal distribution [$D = N(0, 1)$] and an IG distribution of squared uncertainties $u_E^2/\sigma^2 \sim \Gamma^{-1}(\nu/2, \nu/2)$ leads to a scale mixture distribution of errors (Eq. 2), which has the shape of a Student's- t distribution with ν degrees of freedom^{22,23}

$$E/\sigma \sim t(\nu) \quad (18)$$

This scale mixture is a sub-case of the Normal-IG (NIG) distribution used in evidential inference.²⁴ For the squared errors, one gets

$$E^2/\sigma^2 \sim F(1, \nu) \quad (19)$$

where $F(\nu_1, \nu_2)$ is the Fisher-Snedecor (F) distribution²⁰ with degrees of freedom ν_1 and ν_2 .

The squared error datasets have been fitted by a scaled F distribution, and the results are reported in Fig. 2 and Table I. The fits are very good for all sets, except for Set 6, where a minor mode at small errors cannot be accounted for by the F distribution. Here again, the shape parameters cover a wide range, from 0.8 to 10, with very values typical of heavy tails.

It has to be noted that the shape parameter for E^2 is never close to being twice the shape parameter for u_E^2 as expected from the NIG model (Eq. 18). The densities expected from the NIG model are plotted in Fig. 2 (red lines) for comparison with the actual fits and confirm the discrepancy. Therefore, either the generative distribution D is never close to $N(0, 1)$ for the studied datasets, or the datasets are not properly calibrated.

C. Z^2 distributions

The shape parameters for the fit of Z^2 distributions by the same procedure as for E^2 are reported in Table I. The fits (not shown) present the same features as E^2 fits, albeit with typically larger shape parameters, ranging from 0.9 to 20, which is expected from the generative model. Two exceptions are Sets 5 and 8, for which the shape parameter is slightly smaller for Z^2 than for E^2 , a small difference that might not be significant.

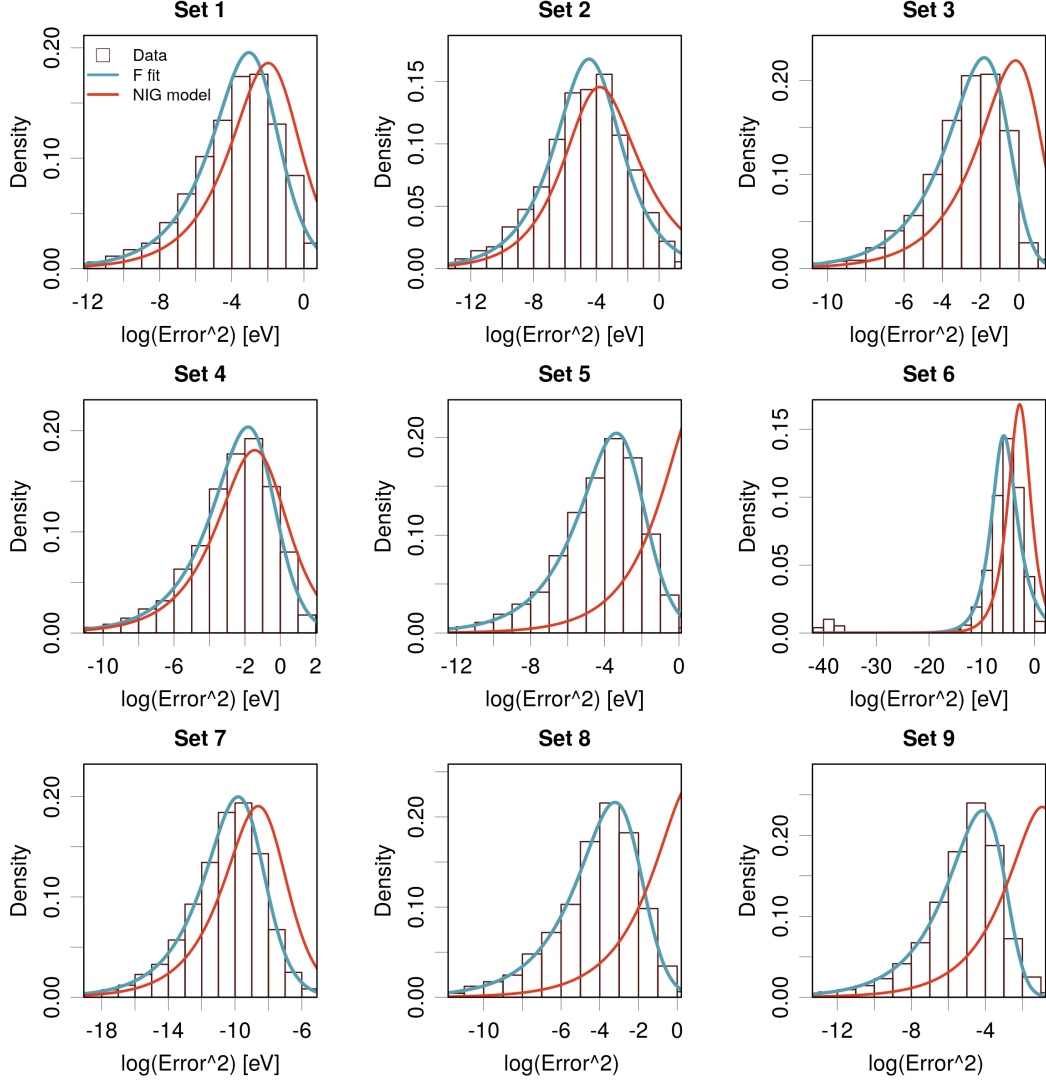


Figure 2. Fit of the squared errors (histogram) by a Fisher-Snedecor $F(1, \nu)$ distribution (blue line). The red curves represent the distributions for NIG models compatible with Fig. 1.

D. Summary

This section showed that it was possible to represent the distribution of u_E^2 sets by an IG distribution with reasonable accuracy, except for bimodal distributions, and that some of these distributions have very small shape parameters indicating very heavy tails. The E^2 and Z^2 distributions were successfully fit by F distributions, some with very small shape parameters indicating heavy tails, but the optimal shape parameters did not conform with the constraints of the NIG model.

The next section demonstrates that the presence of heavy tails in either of these quantities might challenge the reliable estimation and validation of calibration statistics.

IV. NUMERICAL EXPERIMENTS

The characteristic features of the nine datasets presented in the previous sections are now used to design numerical experiments to assess the impact of the distributions tails on the reliability of calibration statistics. A first step is to define tailedness metric independent of model distributions.

A. Alternative tailedness metrics

As shown in the previous section, the shape of the uncertainty and error distributions can be rather well characterized by a shape parameter ν , but one has to take into account that not all datasets are correctly fitted by the model distributions. Besides, for the *IG* and *t* distributions, shape metrics such as skewness and kurtosis are not defined for $\nu \leq 3$ or 4, respectively. One therefore needs distribution-agnostic metrics able to characterize the shape of these distributions.

Considering the asymmetric shape of u_E^2 , E^2 and Z^2 distributions, one might want to describe the length of the upper tail by skewness and/or the heaviness of the tails by kurtosis. For such distributions, these metrics are expected to be correlated²⁵, but they might still provide complementary information.

As one is potentially dealing with heavy-tailed distributions and outliers, it is essential to use robust statistics. β_{GM} is a skewness statistic based on the scaled difference between the mean and median²⁵⁻²⁸, which is robust to outliers, varies between -1 and 1 and is null for symmetric distributions. For kurtosis, κ_{CS} is chosen for the same reasons²⁵⁻²⁸. This is an excess kurtosis, meaning that positive values indicate tails that are heavier than those of the normal distribution. κ_{CS} is not scaled and does not have finite limits.

Fig. 3 shows the correspondence between ν , β_{GM} and κ_{CS} for samples of the *IG* distribution [$X^2 \sim \Gamma^{-1}(\nu/2, \nu/2)$] and *F*-distribution [$X^2 \sim F(1, \nu)$]. There is a monotonous one-to-one correspondence between β_{GM} , κ_{CS} and the ν parameter of the sampled distributions showing that the skewness and kurtosis statistics can be used to replace unambiguously the shape parameter of the model distributions.

Note that the coefficient of variation c_v is often used in ML-UQ studies to quantify the dispersion of uncertainties²⁹, which is also related to the tailedness of their distribution. However, it is not robust and cannot replace the proposed statistics.

Considering that β_{GM} and κ_{CS} are practically exchangeable for the kind of distributions considered here, only β_{GM} is used in the following to characterize the tailedness of the dis-

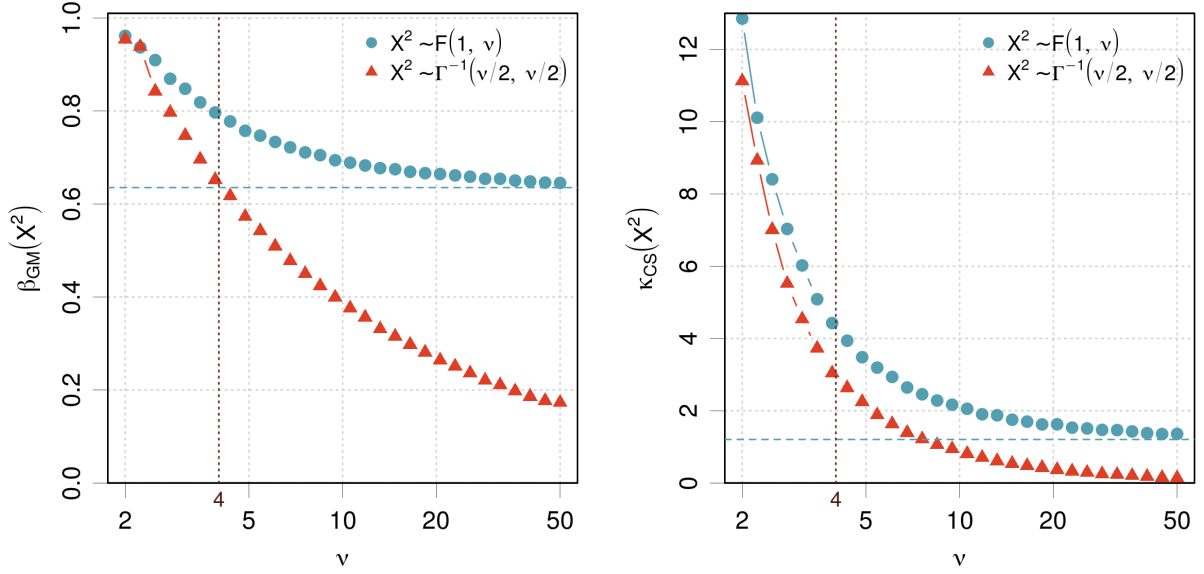


Figure 3. β_{GM} skewness and κ_{CS} kurtosis values for samples (size 5×10^5) issued from Fisher-Snedecor $F(1, \nu)$ distributions (blue dots) and from Inverse-Gamma $\Gamma^{-1}(\nu/2, \nu/2)$ distributions (red triangles). The dashed horizontal line represents the limit for a squared normal variate.

tributions. It provides a conveniently bounded metric.

B. Sensitivity of calibration statistics to heavy-tailed uncertainty and error distributions

To characterize the sensitivity of the RCE and ZMS statistics to the shape of the uncertainty and error distributions, they are estimated for synthetic datasets covering the range of tail statistics observed in the previous sections. $N = 10^3$ synthetic calibrated datasets of size $M = 5000$ are generated using an extension of the NIG model, the TIG model, defined by $u_E^2 \sim \Gamma^{-1}(\nu_{IG}/2, \nu_{IG}/2)$ and $D = t_s(\nu_D)$ where

$$t_s(\nu_D) := t(\nu_D) \times \sqrt{\frac{\nu_D - 2}{\nu_D}} \quad (20)$$

for combinations of parameters such as $\nu_{IG} \in [2, 20]$ and $\nu_D \in [3, 100]$. Smaller values of the parameters have been avoided as they might result in numerical problems. The results are reported in Fig. 4 for RCE vs. $\beta_{GM}(E^2)$ and 1-ZMS vs. $\beta_{GM}(Z^2)$. The mean values and 2σ error bars summarize the sample of N Monte Carlo runs.

The RCE deviates to positive values when $\beta_{GM}(E^2) > 0.85$, and the deviation is increasing with skewness. As the Monte Carlo error bars are not large enough to cover the reference

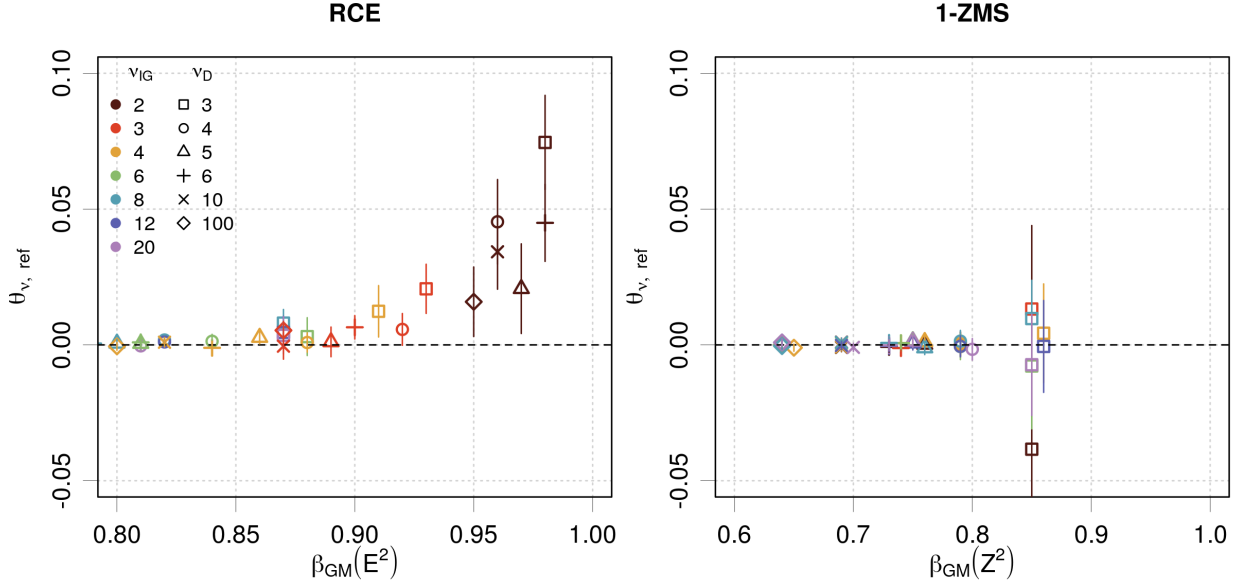


Figure 4. Comparison of the estimated values of RCE and 1-ZMS for a series of datasets generated by TIG models and characterized by their error skewness parameter $\beta_{GM}(E^2)$, or $\beta_{GM}(Z^2)$ for 1-ZMS. The symbols and 2σ error bars summarize a sample of 10^3 Monte Carlo runs.

value (0), one can conclude that the RCE is significantly biased in this area. Note that reformulating the RCE without square roots can help to reduce this bias (see Appendix A). In comparison, the 1-ZMS statistic is better behaved for most of the datasets, and seems to have problems only with the extreme $\nu_D = 3$ case, which corresponds to $\beta_{GM}(Z^2) > 0.8$.

C. Sensitivity of validation statistics to heavy-tailed uncertainty and error distributions

The previous experiment revealed how the RCE and ZMS are sensitive to heavy tails. It occurs that the estimation of confidence intervals for these statistics by bootstrapping has also difficulties in similar conditions, which is put in evidence by the following simulations.

One considers here two scenarios designed to cover the range of distributions observed above, but also to limit the computational cost of the experiments:

- NIG: $u_E^2 \sim \Gamma^{-1}(\nu_{IG}/2, \nu_{IG}/2)$ and $D = N(0, 1)$, with ν_{IG} varying between 2 and 10.
- TIG: $u_E^2 \sim \Gamma^{-1}(3, 3)$ and $D = t_s(\nu_D)$ with ν_D varying between 2.1 and 20.

For each sample ($M = 5000$ with $N = 10^3$ Monte Carlo repeats), the calibration is tested by $|\zeta| \leq 1$ and a probability of validity is estimated as

$$p_{val} = \frac{1}{N} \sum_{i=1}^N \mathbf{1}(|\zeta|_i \leq 1) \quad (21)$$

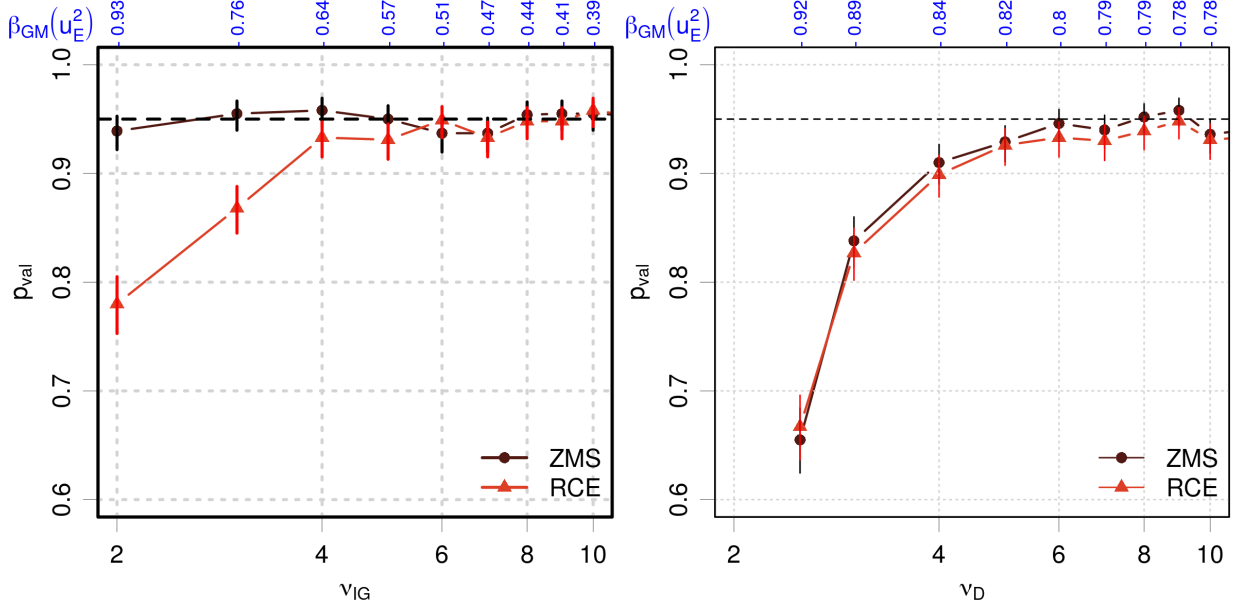


Figure 5. Validation probability of the ZMS and RCE statistics for calibrated datasets generated by two scenarios: (left) NIG with ν_{IG} as parameter of the IG distribution; (right) TIG with ν_D as parameter of the generative $D = t_s$ distribution. The corresponding average values of β_{GM} are reported on the upper axis.

where $\mathbf{1}(x)$ is the indicator function with values 0 when x is false, and 1 when x is true.

The values of p_{val} and their 95% confidence intervals obtained by a binomial model¹¹, are plotted in Fig. 5 for the RCE and ZMS statistics as a function of ν_{IG} or ν_D . The upper axis provides the average β_{GM} statistics for the generated u_E^2 and E^2 samples.

The study of the NIG model shows that the ZMS is not sensitive to ν_{IG} , even for extreme uncertainty distributions, and that it provides intervals that consistently validate 95% of the calibrated synthetic datasets. For the RCE, the validation probability is strongly sensitive to ν_{IG} for values below 4, reaching less than 80% for $\nu_{IG} = 2$.

When considering the TIG model, one sees that both statistics are similarly sensitive to the shape of the generative distribution, and that the validation intervals begin to be unreliable for $\nu_D < 6$ ($\beta_{GM} \geq 0.8$). The validation probability falls to 0.65 for $\nu_D = 2.1$. In this case, when ν_D diminishes, the dispersion of the generated $\langle E^2 \rangle$ or $\langle Z^2 \rangle$ values increases, which is not in itself a problem, but the bootstrapped CIs are unable to capture correctly this effect by being too narrow, i.e. too frequently excluding the true mean value of the distribution.

For further reference one defines safety thresholds for β_{GM} . Based on the data in Figs. 4-5, the limit values above which one can suspect the reliability of the calibration statistics

Variable	β_{GM}	Impacted statistics
u_E^2	0.6	RCE
E^2, Z^2	0.8	RCE, ZMS

Table II. Limits for β_{GM} above which the reliability of the RCE or ZMS calibration statistics should be questioned.

are given in Table II. Note that these values are indicative and result from the distribution shapes observed for the studied datasets. The values for other distribution shapes might differ slightly.

D. Summary

This section was designed to illustrate how the calibration statistics and their validation diagnostic are sensitive to the shape of the uncertainty and error distributions. Two problems were identified.

The first problem is the sensitivity of the mean square (MS) statistic $\langle X^2 \rangle$, which is central to the studied RCE and ZMS, to the presence of outliers or heavy tails in the distribution of X . This is a well known issue, which justifies often the replacement of the root mean squared error RMSE by the more robust mean unsigned error (MUE) in performance analysis^{25,30}. Unfortunately the use of the MS in average calibration statistics derives directly from the probabilistic model linking errors to uncertainties (Eq. 1), and one has to deal with its limitations, unless one is ready to change of uncertainty paradigm, using for instance prediction intervals or distributions.

The second problem is the inability of bootstrapping to provide reliable confidence intervals for $\langle X^2 \rangle$ for heavy-tailed distributions.

The robust skewness (β_{GM}) and kurtosis (κ_{CS}) estimators were proposed and compared as tailedness metrics. Because of their strong correlation, only β_{GM} was retained and safety limits have been derived to help in screening out datasets with potentially unreliable RCE/ZMS values. It has been shown that heavy-tailed uncertainty distributions affect mostly the RCE, while both RCE and ZMS are affected by heavy-tailed error distributions. The ZMS benefits also from the fact that the distribution of Z^2 has often lighter tails than the distribution of E^2 . The next section illustrates these features on the nine example ML-UQ datasets of Sect. III.

Set #	$\beta_{GM}(u_E^2)$	$\beta_{GM}(E^2)$	$\beta_{GM}(Z^2)$
1	0.40	0.82	0.73
2	0.72	0.94	0.83
3	0.66	0.74	0.69
4	0.74	0.82	0.69
5	0.19	0.78	0.79
6	0.50	0.96	0.95
7	0.93	0.98	0.78
8	0.30	0.79	0.78
9	0.30	0.77	0.75

Table III. Robust skewness values for u_E^2 , E^2 and Z^2 . Values above the proposed safety limits (Table II) are in bold type.

V. APPLICATION TO REAL ML-UQ DATASETS

The validation approach presented above is applied to the datasets presented in Sec. III. First, the datasets are characterized by their skewness to validate the analysis of shape parameters reported above. Then, the comparison of calibration diagnostics for the RCE and ZMS is analyzed according to the skewness values.

A. Skewness analysis

The first step is to assess the tailedness of the uncertainty, error and z-score distributions to reveal potentially problematic datasets. The corresponding β_{GM} values are reported in Table III.

The skewness values indicate that some distributions present heavy tails. For uncertainties, $\beta_{GM}(u_E^2)$ exceed 0.6 for Sets 2, 3, 4, and 7. This list conforms to the shape analysis of Table I, except for Set 6, which had a very small ν parameter but has a moderate skewness. For the errors, the largest values occur for Sets 1, 2, 4, 6 and 7, a list where the shape analysis of Table I would have added Set 5. For the z-scores, only two sets are screened out, Sets 2 and 6, while Sets 5 and 6 have small ν values. The correspondence between the previous shape analysis and the skewness screening is not perfect, which reflects the imperfect quality of the distributions fits provided by the IG and F models. According to the present analysis, Sets 1, 2, 3, 4, 6 and 7 are potentially problematic, Set 1 being very close to the limit.

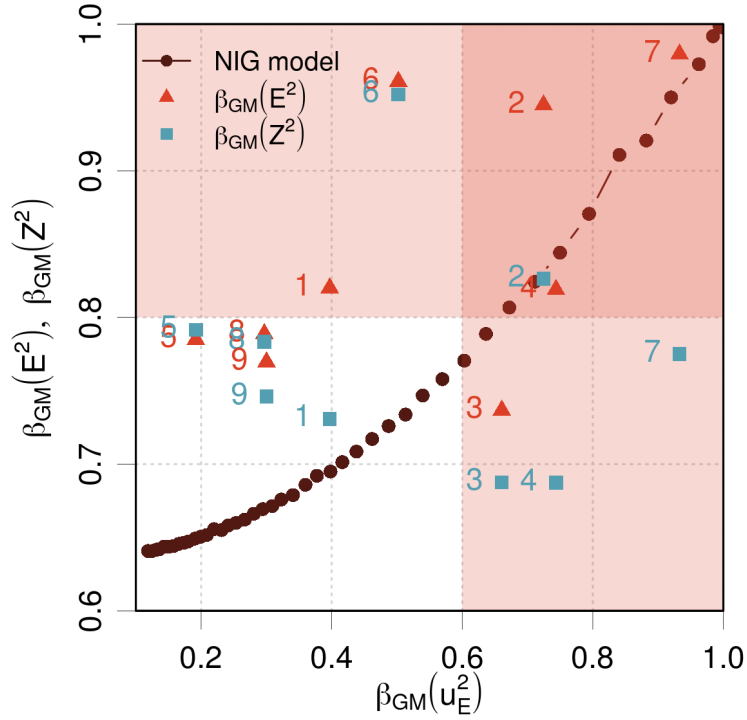


Figure 6. Skewness analysis of the application datasets. The black dots figure the NIG model for $2 \leq \nu \leq 20$. The colored areas signal the values that might be associated with problems.

A graphical summary of the skewness analysis is provided in Fig. 6, where $\beta_{GM}(E^2)$ is plotted against $\beta_{GM}(u_E^2)$ for the nine datasets (red triangles) and for the NIG model ($2 \leq \nu \leq 20$; black dots). One sees directly that only Sets 5, 8 and 9 are in the safe area for both statistics, although they lie close to the E^2 skewness limit. All the other sets have a skewness value that might be problematic for at least one of u_E^2 or E^2 . It is also noteworthy that most $\beta_{GM}(E^2)$ values (except for Sets 3, 4 and 7) exceed what should be expected from the NIG model, confirming the shape analysis of Sect. III.

The blue squares depict the values for $\beta_{GM}(Z^2)$: except for Sets 2 and 6, they all lie below the safety limit (0.8), and for Set 2 the value is much closer to the limit than $\beta_{GM}(E^2)$. This indicates that the ZMS is much less likely to be affected by estimation problems than the RCE, but might still be challenged by data such as Sets 2 and 6.

B. Comparison of validation scores

The statistics and bootstrapped confidence intervals have been estimated for the RCE and ZMS for all datasets with 10^4 bootstrap replicates. The resulting values and validation scores are reported in Table IV. It is clear from these results that average calibration is not satisfied

$\vartheta = RCE; \vartheta_{ref} = 0$					$\vartheta = ZMS; \vartheta_{ref} = 1$				
Set	ϑ_{est}	b_{BS}	I_{BS}	ζ_{RCE}	Set	ϑ_{est}	b_{BS}	I_{BS}	ζ_{ZMS}
1	0.019	2.2e-04	[-0.021, 0.055]	0.47	1	0.96	-2.7e-04	[0.87, 1.11]	-0.27
2	-0.039	5.9e-04	[-0.106, 0.020]	-0.66	2	0.89	-7.3e-04	[0.80, 0.999]	-1.01
3	-0.0075	-2.1e-04	[-0.054, 0.040]	-0.16	3	1.12	9.4e-05	[1.05, 1.2]	1.73
4	0.055	-3.9e-04	[-0.0025, 0.12]	0.96	4	1.23	-6.4e-04	[1.16, 1.3]	3.50
5	0.099	1.4e-04	[0.057, 0.14]	2.33	5	0.85	1.3e-04	[0.78, 0.93]	-1.84
6	0.092	9.9e-04	[0.00079, 0.16]	1.01	6	0.98	-6.2e-04	[0.85, 1.15]	-0.10
7	-0.26	5.5e-03	[-0.68, -0.0012]	-1.00	7	0.97	2.6e-04	[0.94, 1.01]	-0.69
8	0.046	1.3e-05	[0.0082, 0.077]	1.22	8	0.93	3.4e-04	[0.87, 0.99]	-1.12
9	-0.013	2.1e-04	[-0.072, 0.027]	-0.33	9	0.97	2.5e-04	[0.90, 1.08]	-0.26

Table IV. RCE and ZMS statistics and their validation results. The bold ζ_x values indicate calibrated sets, where $|\zeta_x| \leq 1$.

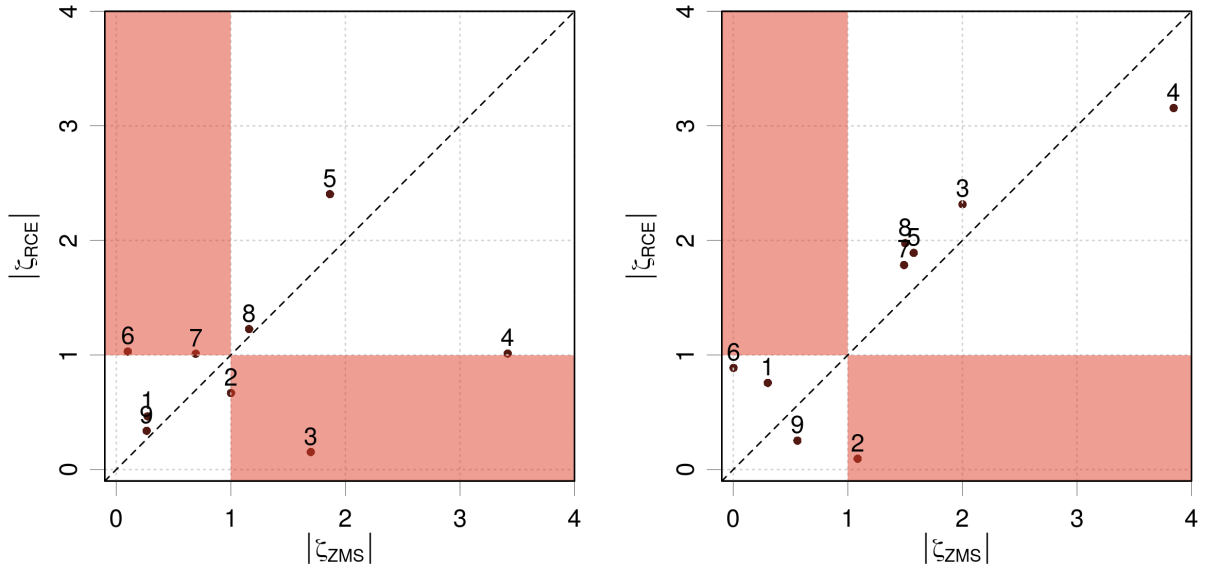


Figure 7. Comparison of the absolute ζ -scores for ZMS and RCE: (left) the original datasets; (right) after removal of the 5% largest uncertainties. The symbols represent the set numbers in Table IV. The colored areas contain the disagreeing validation results.

by all datasets and, more problematically, that the diagnostic depends notably on the choice of statistic.

Comparison of the absolute ζ -scores for ZMS and RCE across the nine datasets shows a contrasted situation [Fig. 7(left)]:

- Points close to the identity line and more globally in uncolored areas, are the datasets for which both statistics agree on the calibration diagnostic, i.e. positive for Sets 1 and 9, and negative for Set 5 and 8.
- Sets 6 and 7 are validated by the ZMS and rejected by the RCE, although very close to the limit.
- Finally, Sets 2, 3 and 4 are validated by RCE and rejected by ZMS.

Globally, the statistics disagree on more than half of the datasets, which is surprising for two statistics deriving analytically from the same generative model (Eq. 1). Considering that the RCE ignores the pairing of uncertainties and errors, one could have expected it to be more forbidding than the ZMS, which is the case for Sets 2, 3 and 4, but not for Set 6 (maybe also for Sets 5 and 7).

It is remarkable that the five sets for which a disagreement between RCE and ZMS is observed (Sets 2, 3, 4, 6 and 7) are those with the largest skewness values for u_E^2 (Table III, Fig. 6), with $\beta_{GM}(u_E^2) \geq 0.6$, except for Set 6, as shown in Fig. 6(left). This suggests that the upper tail of the uncertainty distribution plays a major role in this disagreement. Sets 2, 4, 6 and 7 present also $\beta_{GM}(E^2) \geq 0.8$, which might point to problematic error distributions.

The impact of the tails of the uncertainty and error distributions is assessed in the next section.

C. Impact of the distributions tails

In order to better understand the discrepancy of the validation results by RCE and ZMS, one needs to consider the sensitivity of these statistics to the uncertainty distributions, and notably to the large, sometimes outlying, values, as suggested by the skewness analysis. In the z-scores, these large uncertainty values are likely to contribute to small absolute values of Z having a small impact on the ZMS, while they are likely to affect significantly the estimation of the RCE. This hypothesis is tested on the nine datasets by a decimation experiment, where both statistics are estimated on datasets iteratively pruned from their largest uncertainties.

The deviations of the ZMS and RCE scores from their value for the full dataset are estimated for an iterative pruning (decimation) of the datasets from their largest uncertainties, as performed in confidence curves³¹. The values of $\Delta_{RCE} = RCE_k - RCE_0$ and $\Delta_{ZMS} = ZMS_k - ZMS_0$ for a percentage k of discarded data varying between 0 and 10 % are shown

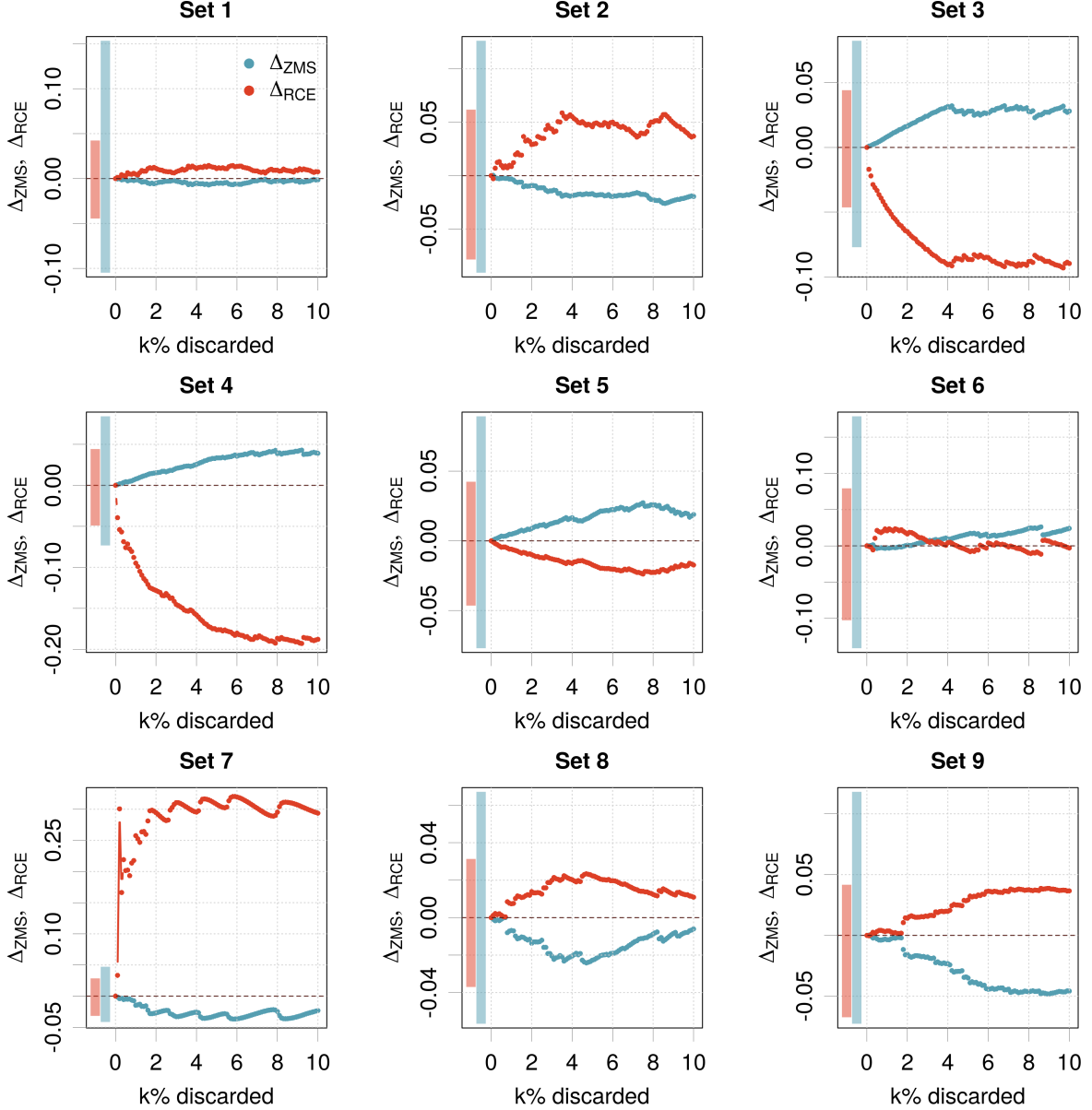


Figure 8. Variation of the RCE and ZMS statistics according to the percentage k of largest uncertainties removed from the datasets. The vertical colored bars represent 95% confidence intervals on the statistics for the full datasets.

in Fig. 8, where zero-centered bootstrapped 95% CIs for both statistics are displayed as vertical bars to assess the amplitude of the deviations.

It appears that in all the cases ZMS is less or as sensitive as RCE to the large extremal uncertainty values and that its decimation curve always strays within the limits of the corresponding CI. For RCE, one can find cases where it is more sensitive than ZMS but lies within the limits of the CI (Sets 2 and 6) and cases where it strays beyond the limits of the CI (Sets 3, 4 and 7). These five cases are precisely those where the RCE diagnostic differs the most from the ZMS (Sect. V B). This sensitivity test confirms the hypothesis that RCE is more sensitive

than ZMS to the upper tail of the uncertainty distribution, to a point where its estimation might become unreliable.

For some sets (2, 3, 6 and 7) a small percentage (1-4 %) of the largest uncertainties affects the Δ_{RCE} statistic, after which one observes a sharp change of slope, and the curves becomes a reflected image of the Δ_{ZMS} statistic. These uncertainties might therefore be considered as outlying values. By contrast, one observes for Set 4 a smooth transition, which suggest that the shape of the tail is involved, rather than a few extreme uncertainty values.

The sensitivity of the ζ -scores to the removal of the 5 % largest uncertainties is shown in Fig. 7(right). One can expect from this truncation a better agreement of ZMS and RCE for those datasets with heavy u_E tails. The agreement is indeed notably improved for Set 3, 4 and 7.

Surprisingly, the ζ_{RCE} values for Sets 2 and 6 do not follow the same trend, with a deterioration for Set 2 and no notable change for Set 6. Note that these are the sets for which the Δ_{RCE} curve does *not* stray notably out of the corresponding CI limits. The main reason for the discrepancy of validation metrics for Sets 2 and 6 is therefore not the shape of the uncertainty distributions, which leads us to the error distributions.

Both datasets present very large error skewness values $\beta_{GM}(E^2)$ (0.92 and 0.96) , well above the safety limit of 0.8. The skewness of z-scores $\beta_{GM}(Z^2)$ for these sets (0.83 and 0.95), although smaller than $\beta_{GM}(E^2)$, are also above the safety limit. It is therefore difficult to conclude on the average calibration of Sets 2 and 6, as both the RCE and ZMS are likely to be affected by the heavy-tails of the E^2 and Z^2 distributions, respectively.

D. Additional datasets

After the completion of this study, Jacobs *et al.*³² published an ensemble of 33 datasets of ML materials properties, with predictions by random forest models and calibrated uncertainty estimates. These new datasets offer a unique opportunity to test the generalizability of the analysis presented above. For this, one will first analyze the skewness of the Z^2 distributions and then observe the discrepancy of the RCE and ZMS calibration statistics.

The prediction uncertainties in these datasets have been calibrated *pos-hoc*, by a polynomial transformation. The parameters of the calibration polynomial have been estimated by NLL minimization, which, in this setup, is equivalent to an optimization of the ZMS to its target value (Eq. 12). It is therefore expected that all the datasets have good ZMS statistics. Skewness and calibration statistics are reported in Table V-VI of Appendix B. Due to

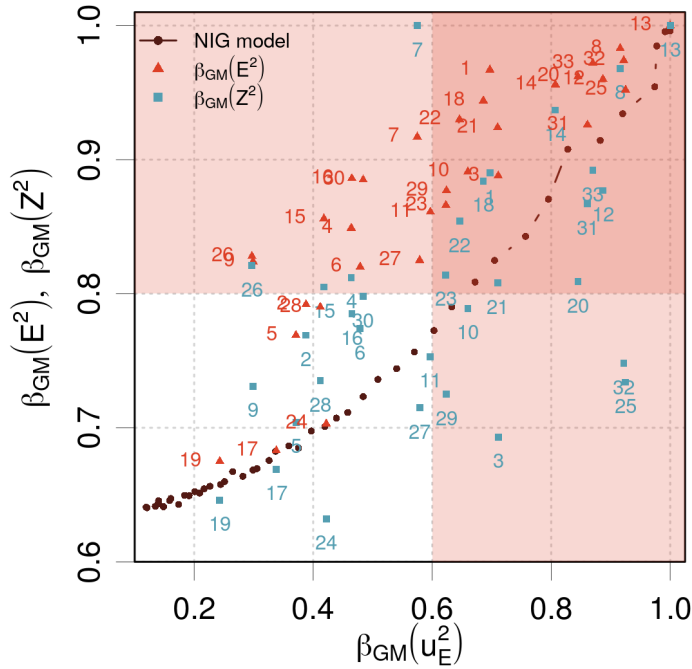


Figure 9. Same as Fig. 6 for Jacobs *et al.*³² 33 datasets.

aberrant data and statistics, Set 13 is reported, but excluded from the discussions.

1. Skewness analysis

All datasets in the colored areas in Fig. 9 are likely to have calibration statistics influenced by heavy tails and/or outliers: about half of the datasets have heavy-tailed u_E^2 distributions, while more than 5 out of 6 have heavy E^2 tails (red triangles); many of them present both features. Only 6 datasets are in the “safe” area where the estimation of mean squared statistics should not be too biased (2, 5, 17, 19, 24, 28). It is also remarkable that a few sets (17, 19, 24, 25 and 31) lie close to the NIG model line, indicating that they might be associated with a quasi-normal generative distribution. However, most of the points lie far above the NIG model line, showing that their generative distributions are far from being normal. Here again, the Z^2 distributions (blue squares) are globally less problematic than the error distributions, but only a little more than half of the cases lies below the $\beta_{GM}(Z^2) = 0.8$ threshold. Set 7 presents an awkward scenario where the skewness of Z^2 is larger than the skewness of E^2 , certainly due to the presence of outlying error values, as noted in Appendix B. Only two sets (Sets 19 and 24) have $\beta_{GM}(Z^2)$ values compatible with a normal distribution (0.64). This larger panel of cases confirms the previous observations that many ML-UQ datasets

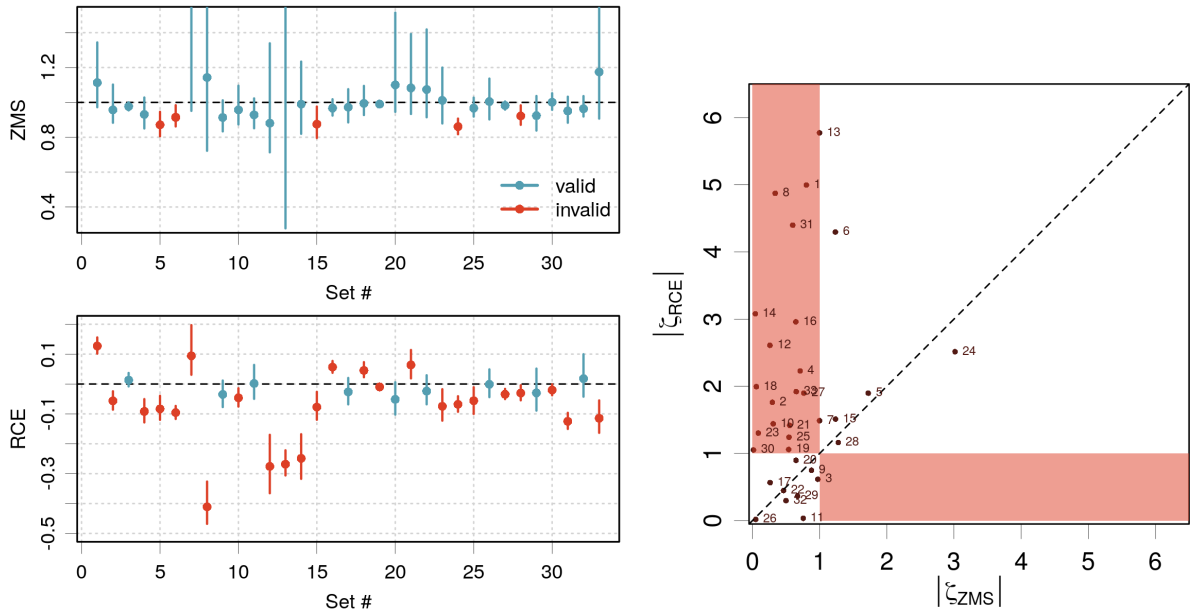


Figure 10. Comparison of ZMS and RCE calibration and validation scores for Jacobs *et al.*³² 33 datasets. (left) ZMS and RCE calibration statistics with bootstrapped 95% confidence intervals. Red intervals do not cover the target value. (right) Same as Fig. 7 .

present distributions that might be challenging for the reliability of variance-based calibration statistics.

In their analysis, Jacobs *et al.*³² associate calibration with the standard-normality of z -scores (see for instance Sects. 2.3 and 3.2 of their article). If this were the case, very few of the 33 datasets should be considered as calibrated. In fact, and according to the generative model (Eq. 1), calibration is assessed by unbiasedness ($\langle Z \rangle = 0$) and unit ZMS ($\langle Z^2 \rangle = 1$) or unit variance ($\text{Var}(Z) = 1$), without reference to the shape of the distribution. The NLL score minimized for the calibration of uncertainties cannot ensure the normality of z -scores, because it does not involve nor constrain moments higher than the second order.

2. Comparison of calibration and validation scores

Fig. 10(left) presents the ZMS and RCE calibration statistics with their bootstrapped 95% confidence intervals. Considering the ZMS, one sees that Sets 7 (and 13), despite huge ZMS values, are validated due to very wide confidence intervals. This raises an alert on the blind use of validation statistics such as ζ -scores for heavy-tailed distributions or datasets with outliers. One can also see that Sets 5, 6, 15, 24 and 28 have invalidated ZMS values. These datasets should therefore not be considered as calibrated.

The RCE values show a much larger panel of invalidated datasets. This discrepancy

between ZMS and RCE is problematic and reflects the unreliability of these statistics for heavy-tailed uncertainty and/or error distributions. The statistics agree for Sets 3, 5, 6, 9, 11, 15, 17, 20, 22, 24, 26, 28, 29 and 32, i.e. less than half of the cases (14 over 33). The majority of these agreements correspond to datasets with $\beta_{GM}(Z^2) \leq 0.8$. It is therefore legitimate to question the validity of the calibration statistics for the other, heavy-tailed, datasets.

Another way to look at the disagreement of the RCE and ZMS statistics is to compare their zeta scores. Fig. 10(right) comforts the skewness analysis. Points close to the diagonal are those for which the calibration diagnostics (either positive or negative) agree. Most of the sets in the safe area for skewness (Fig. 9) fall in this case (5, 17, 24 and 28). But, globally, the calibration statistics disagree, as observed also in Fig. 10(left).

VI. CONCLUSIONS

This study used the RCE and ZMS average calibration statistics to illustrate the impact of heavy-tailed uncertainty and/or error distributions on the reliability of calibration statistics. These statistics have been used because they have well defined reference values for statistical validation, which is not the case of the more popular bin-based statistics, such as the ENCE.

Discrepancies of validation diagnostic was observed between both statistics for an ensemble of datasets extracted from the recent ML-UQ literature for regression tasks in materials and chemical sciences. This anomaly has been elucidated by showing that the RCE is very sensitive to the upper tail of the uncertainty distribution, and notably to the presence of outliers, which has been proven by a decimation experiment (5 cases out of 9). Moreover, error sets with heavy tails can also be challenging for the RCE (5 cases). The distribution of z-scores ($Z = E/u_E$) appeared to be less problematic, although some heavy-tailed Z distributions have been observed (2 cases).

Two underlying problems contribute to this state of affairs: (1) strong sensitivity of the Mean Squares statistic to the presence of heavy-tails and outliers; and (2) our inability to design reliable confidence intervals with a prescribed coverage for the mean of variables with heavy-tailed distributions (u_E^2 , E^2 and Z^2). Bootstrapping is presently the best approach to CI estimation for the mean of non-normal variables, and numerical experiments have shown that it fails in conditions representative of the studied datasets.

A major consequence of these observations is that average calibration statistics based on the comparison of $MSE = \langle E^2 \rangle$ to $MV = \langle u_E^2 \rangle$ should not be blindly relied upon for the kind of datasets found in ML-UQ regression problems. The RCE is affected by both MSE

and MV sensitivity to heavy tails. In contrast, the ZMS statistic has fewer reliability issues and should therefore be the statistic of choice for average calibration testing. Nevertheless, it should not be expected to be fully reliable.

In this context, it is important to be able to screen out problematic datasets. It has been shown that a robust skewness statistic (β_{GM}) can be used for this, and safety thresholds have been defined for the u_E^2 , E^2 and Z^2 distributions. The reliability of the RCE and ZMS statistics for datasets with values exceeding these limits has to be questioned.

A temptation would be to ignore altogether average calibration statistics and to focus on conditional calibration. As the RCE, the popular UCE and ENCE statistics implement the comparison of MV to MSE , but, being bin-based, one might expect them to be less susceptible to the above-mentioned sensitivity issue when the binning variable is u_E (*consistency testing*²). Unfortunately, even if binning solves the tailedness problem for $\langle u_E^2 \rangle$ for most of the bins, this is not the case for $\langle E^2 \rangle$, leaving these conditional calibration statistics with the same reliability problem as the RCE. This also applies to the local ZMS analysis. The problem of conditional calibration statistics will be further explored in a forthcoming article.

In *post hoc* calibration, scaling factors for the uncertainties can be derived from the ZMS (σ scaling³³, BVS^{34,35}, polynomial scaling^{18,32}) or from the UCE³⁴. So, by extension, the outlined problems also affect *post-hoc* calibration procedures based on statistics related to the RCE, ENCE or ZMS (for instance the NLL). Those methods parameterized on datasets with heavy uncertainty and/or error tails might also be unreliable.

An ensemble of 33 datasets³², published after the completion of this study, has been included to validate these conclusions and it fully confirms them. One can therefore be confident that heavy tailed distribution of uncertainties, errors and z-scores are presently a notable feature of ML materials properties datasets which has to be seriously taken into account.

One can envision three paths out of this lack of reliability of calibration statistics:

1. The reduction of the problematic tails of uncertainty and error distributions can be handled to some extent by iterative learning, i.e. by iteratively feeding the data with the largest absolute errors and uncertainties to the training algorithm until the problem subsides³⁶.
2. For datasets with uncontrollable heavy tails, one might have to abandon formal validation and to rely on graphical methods to derive a qualitative calibration diagnostic^{11,12}.

3. A change of uncertainty metric, using prediction intervals or distributions instead of standard deviations, would enable a better handling of heavy tails and seems presently to be the most promising alternative to recover a sound statistical validation framework for calibration.

ACKNOWLEDGMENTS

I warmly thank J. Busk for providing the QM9 dataset and R. Jacobs for his help with the “33 datasets”.

AUTHOR DECLARATIONS

Conflict of Interest

The author has no conflicts to disclose.

CODE AND DATA AVAILABILITY

The code and data to reproduce the results of this article are available at https://github.com/ppernot/2024_RCE/releases/tag/v4.0 and at Zenodo (<https://doi.org/10.5281/zenodo.13341150>). The 33 datasets of Jacobs *et al.*³² are accessible in a FigShare depository³⁷.

REFERENCES

- ¹D. Levi, L. Gispan, N. Giladi, and E. Fetaya. [Evaluating and Calibrating Uncertainty Prediction in Regression Tasks](#). *Sensors*, 22:5540, 2022.
- ²P. Pernot. [Calibration in machine learning uncertainty quantification: Beyond consistency to target adaptivity](#). *APL Mach. Learn.*, 1:046121, 2023.
- ³T. Gneiting and A. E. Raftery. [Strictly Proper Scoring Rules, Prediction, and Estimation](#). *J. Am. Stat. Assoc.*, pages 359–378, 2007.
- ⁴K. Tran, W. Neiswanger, J. Yoon, Q. Zhang, E. Xing, and Z. W. Ulissi. [Methods for comparing uncertainty quantifications for material property predictions](#). *Mach. Learn.: Sci. Technol.*, 1:025006, 2020.
- ⁵M. H. Rasmussen, C. Duan, H. J. Kulik, and J. H. Jensen. [Uncertain of uncertainties? A comparison of uncertainty quantification metrics for chemical data sets](#). *J. Cheminf.*, 15:1–17, 2023.

- ⁶J. Wellendorff, K. T. Lundgaard, K. W. Jacobsen, and T. Bligaard. [mBEEF: An accurate semi-local bayesian error estimation density functional](#). *J. Chem. Phys.*, 140:144107, 2014.
- ⁷P. Pernot and F. Cailliez. [A critical review of statistical calibration/prediction models handling data inconsistency and model inadequacy](#). *AIChE J.*, 63:4642–4665, 2017.
- ⁸V. Kuleshov, N. Fenner, and S. Ermon. [Accurate uncertainties for deep learning using calibrated regression](#). In J. Dy and A. Krause, editors, *Proceedings of the 35th International Conference on Machine Learning*, volume 80 of *Proceedings of Machine Learning Research*, pages 2796–2804. PMLR, 10–15 Jul 2018. URL: <https://proceedings.mlr.press/v80/kuleshov18a.html>.
- ⁹P. Pernot. [Properties of the ENCE and other MAD-based calibration metrics](#). *arXiv:2305.11905*, May 2023.
- ¹⁰BIPM, IEC, IFCC, ILAC, ISO, IUPAC, IUPAP, and OIML. [Evaluation of measurement data - Guide to the expression of uncertainty in measurement \(GUM\)](#). Technical Report 100:2008, Joint Committee for Guides in Metrology, JCGM, 2008. URL: http://www.bipm.org/utils/common/documents/jcgm/JCGM_100_2008_F.pdf.
- ¹¹P. Pernot. [The long road to calibrated prediction uncertainty in computational chemistry](#). *J. Chem. Phys.*, 156:114109, 2022.
- ¹²P. Pernot. [Prediction uncertainty validation for computational chemists](#). *J. Chem. Phys.*, 157:144103, 2022.
- ¹³J. Busk, M. N. Schmidt, O. Winther, T. Vegge, and P. B. Jørgensen. [Graph neural network interatomic potential ensembles with calibrated aleatoric and epistemic uncertainty on energy and forces](#). *Phys. Chem. Chem. Phys.*, 25:25828–25837, 2023.
- ¹⁴W. Zhang, Z. Ma, S. Das, T.-W. Weng, A. Megretski, L. Daniel, and L. M. Nguyen. [One step closer to unbiased aleatoric uncertainty estimation](#). *arXiv:2312.10469*, December 2023.
- ¹⁵T. Gneiting, F. Balabdaoui, and A. E. Raftery. [Probabilistic forecasts, calibration and sharpness](#). *J. R. Statist. Soc. B*, 69:243–268, 2007.
- ¹⁶T. J. DiCiccio and B. Efron. [Bootstrap confidence intervals](#). *Statist. Sci.*, 11:189–212, 1996. URL: <https://www.jstor.org/stable/2246110>.
- ¹⁷P. Pernot. [Validation of uncertainty quantification metrics: a primer based on the consistency and adaptivity concepts](#). *arXiv:2303.07170*, 2023. *arXiv:2303.07170*.
- ¹⁸G. Palmer, S. Du, A. Politowicz, J. P. Emory, X. Yang, A. Gautam, G. Gupta, Z. Li, R. Jacobs, and D. Morgan. [Calibration after bootstrap for accurate uncertainty quantification in regression models](#). *npj Comput. Mater.*, 8:115, 2022.

- ¹⁹J. Busk, P. B. Jørgensen, A. Bhowmik, M. N. Schmidt, O. Winther, and T. Vegge. [Calibrated uncertainty for molecular property prediction using ensembles of message passing neural networks](#). *Mach. Learn.: Sci. Technol.*, 3:015012, 2022.
- ²⁰M. Evans, N. Hastings, and B. Peacock. *Statistical Distributions*. Wiley-Interscience, 3rd edition, 2000.
- ²¹M. L. Delignette-Muller and C. Dutang. [fitdistrplus: An R package for fitting distributions](#). *J Stat Softw*, 64(4):1–34, 2015.
- ²²D. F. Andrews and C. L. Mallows. [Scale mixtures of normal distributions](#). *Journal of the Royal Statistical Society. Series B (Methodological)*, 36:99–102, 1974. URL: <http://www.jstor.org/stable/2984774>.
- ²³S. T. B. Choy and J. S. K. Chan. [Scale mixtures distributions in statistical modelling](#). *Aust. N.Z. J. Stat.*, 50:135–146, 2008.
- ²⁴A. Amini, W. Schwarting, A. Soleimany, and D. Rus. [Deep Evidential Regression](#). *arXiv:1910.02600*, October 2019.
- ²⁵P. Pernot and A. Savin. [Using the Gini coefficient to characterize the shape of computational chemistry error distributions](#). *Theor. Chem. Acc.*, 140:24, 2021.
- ²⁶E. L. Crow and M. M. Siddiqui. [Robust estimation of location](#). *J. Am. Stat. Assoc.*, 62:353–389, 1967.
- ²⁷R. A. Groeneveld and G. Meeden. [Measuring skewness and kurtosis](#). *The Statistician*, 33:391–399, 1984. URL: <http://www.jstor.org/stable/2987742>.
- ²⁸M. Bonato. [Robust estimation of skewness and kurtosis in distributions with infinite higher moments](#). *Financ Res Lett*, 8:77–87, 2011.
- ²⁹G. Scalia, C. A. Grambow, B. Pernici, Y.-P. Li, and W. H. Green. [Evaluating scalable uncertainty estimation methods for deep learning-based molecular property prediction](#). *J. Chem. Inf. Model.*, 60:2697–2717, 2020.
- ³⁰P. Pernot and A. Savin. [Probabilistic performance estimators for computational chemistry methods: the empirical cumulative distribution function of absolute errors](#). *J. Chem. Phys.*, 148:241707, 2018.
- ³¹P. Pernot. [Confidence curves for UQ validation: probabilistic reference vs. oracle](#). *arXiv:2206.15272*, June 2022.
- ³²R. Jacobs, L. E. Schultz, A. Scourtas, K. J. Schmidt, O. Price-Skelly, W. Engler, I. Foster, B. Blaiszik, P. M. Voyles, and D. Morgan. [Machine Learning Materials Properties with Accurate Predictions, Uncertainty Estimates, Domain Guidance, and Persistent Online Accessibility](#). *arXiv:2406.15650*, June 2024.

- ³³M.-H. Laves, S. Ihler, J. F. Fast, L. A. Kahrs, and T. Ortmaier. [Well-calibrated regression uncertainty in medical imaging with deep learning](#). In T. Arbel, I. Ben Ayed, M. de Bruijne, M. Descoteaux, H. Lombaert, and C. Pal, editors, *Proceedings of the Third Conference on Medical Imaging with Deep Learning*, volume 121 of *Proceedings of Machine Learning Research*, pages 393–412. PMLR, 06–08 Jul 2020. URL: <https://proceedings.mlr.press/v121/laves20a.html>.
- ³⁴L. Frenkel and J. Goldberger. [Calibration of a regression network based on the predictive variance with applications to medical images](#). In *2023 IEEE 20th International Symposium on Biomedical Imaging (ISBI)*, pages 1–5. IEEE, 2023.
- ³⁵P. Pernot. [Can bin-wise scaling improve consistency and adaptivity of prediction uncertainty for machine learning regression ?](#) *arXiv:2310.11978*, October 2023.
- ³⁶P. Pernot, B. Huang, and A. Savin. [Impact of non-normal error distributions on the benchmarking and ranking of Quantum Machine Learning models](#). *Mach. Learn.: Sci. Technol.*, 1:035011, 2020.
- ³⁷D. Morgan and R. Jacobs. [Machine Learning Materials Properties with Accurate Predictions, Uncertainty Estimates, Domain Guidance, and Persistent Online Accessibility - FigShare dataset](#). 6 2024.

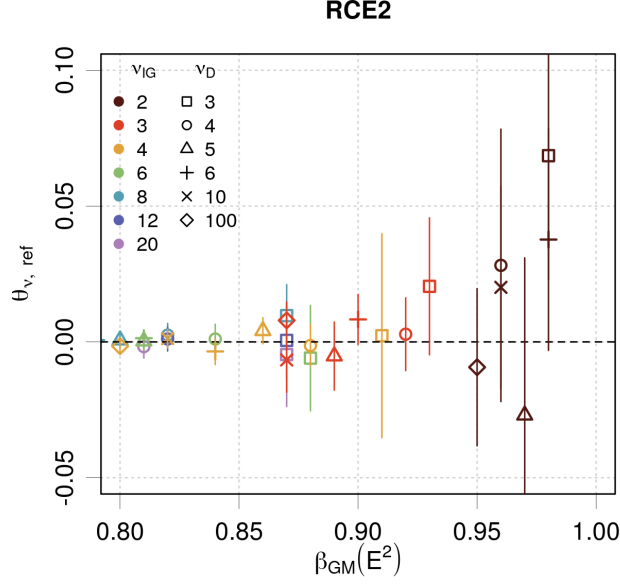


Figure 11. Estimated values of an alternative RCE formulation for a series of datasets generated by TIG models and characterized by the error skewness parameter $\beta_{GM}(E^2)$.

Appendix A: An alternative formulation of RCE

The biased estimation of the RCE as defined by Eq. II A for heavy-tailed uncertainty and error distributions can be reduced by expressing it as

$$RCE2 = \frac{MV - MSE}{MV} \quad (A1)$$

where the mean variance (MV) and mean squared errors (MSE) are used instead of their square roots.

Simulations with the same setup as in Sect. IV B were performed for the RCE2 statistic. The results are reported in Fig. 11.

When compared to the results for the original RCE [Fig. 4(left)], two features are remarkable: (1) the mean values present also deviations increasing with β_{GM} , but with positive or negative signs; and (2) the Monte Carlo 2σ error bars now cover the reference value, so that there is no systematic bias for RCE2.

Appendix B: Statistics of Jacobs *et al.* datasets

Skewness and calibration statistics for the 33 datasets of Jacobs *et al.*³² are presented in Table V-VI.

The uncertainties u_E are taken from the `model_error_leaveout_calibrated.csv` files, and the errors E from the `residuals_leaveout.csv` files. Note that a few datasets present anomalous data, such as non-positive uncertainties, perfectly null errors or remarkable outliers:

- Set 1 has 10% of null errors;
- Set 6 has 1 non-positive uncertainty;
- Set 7 has 5 outlying negative errors leading to a very large ZMS value;
- Set 13 has many non-positive uncertainties and null errors.

Null errors might result from the prediction of properties with physical limits (such as band gaps that should be positive or null). Their occurrence is only problematic for the logarithmic representation of error or z-scores distributions, such as in Figs 2. These data are *not* excluded from the statistical analysis. Similarly, the outliers of Set 7 have been kept. *A contrario*, non-positive uncertainties are most likely an artifact of an unconstrained NLL calibration procedure, and they have systematically been filtered-out for the processing of these datasets. Note that for Set 13, the ZMS statistic is numerically aberrant, even after filtering.

#	Name	M	$n_0(u_E)$	$n_0(E)$	$\beta_{GM}(u_E^2)$	$\beta_{GM}(E^2)$	$\beta_{GM}(Z^2)$	ZMS	RCE
1	bandgap_expt	30150	0	3070	0.7	0.97	0.89	1.11	0.13
2	concrete	5150	0	0	0.39	0.79	0.77	0.96	-0.06
3	debyeT_aflow	24480	0	0	0.71	0.89	0.69	0.98	0.01
4	dielectric	5280	0	0	0.46	0.85	0.81	0.93	-0.09
5	diffusion	2040	0	0	0.37	0.77	0.70	0.87	-0.08
6	double_perovskite_gap	6529	1	0	0.48	0.82	0.77	0.91	-0.1
7	elastic_tensor	5905	0	0	0.57	0.92	1.00	8.2e2	0.09
8	exfoliation_E	3180	0	0	0.92	0.98	0.97	1.14	-0.41
9	hea_hardness	1850	0	0	0.30	0.82	0.73	0.91	-0.03
10	heusler	5405	0	0	0.66	0.89	0.79	0.96	-0.05
11	Li_conductivity	1860	0	0	0.60	0.86	0.75	0.93	0.00
12	metallicglass_Dmax	4990	0	3	0.89	0.96	0.88	0.88	-0.28
13	metallicglass_Rc	8412	2213	7825	1.00	1.00	1.00	1.7e+26	-0.27
14	metallicglass_Rc_LLM	1485	0	8	0.81	0.96	0.94	0.99	-0.25
15	Mg_alloy	1825	0	0	0.42	0.86	0.81	0.88	-0.08
16	oxide_vacancy	24570	0	0	0.46	0.89	0.79	0.97	0.06
17	perovskite_ASR	1445	0	0	0.34	0.68	0.67	0.97	-0.03

Table V. Datasets statistics: M (size), $n_0(u_E)$ (number of non-positive uncertainties), $n_0(E)$ (number of null errors), $\beta_{GM}(u_E^2)$, $\beta_{GM}(E^2)$, $\beta_{GM}(Z^2)$, ZMS, ζ_{ZMS} , RCE and ζ_{RCE} . For skewness statistics, the bold data point to potentially problematic values. For calibration statistics the bold values point to invalid calibration.

#	Name	M	$n_0(u_E)$	$n_0(E)$	$\beta_{GM}(u_E^2)$	$\beta_{GM}(E^2)$	$\beta_{GM}(Z^2)$	ZMS	RCE
18	perovskite_conductivity	36150	0	0	0.69	0.94	0.88	0.99	0.05
19	perovskite_formationE	28938	0	1	0.24	0.67	0.65	0.99	-0.01
20	perovskite_Habs	3975	0	0	0.85	0.96	0.81	1.1	-0.05
21	perovskite_Opband	14560	0	0	0.71	0.92	0.81	1.08	0.06
22	perovskite_stability	14220	0	0	0.65	0.93	0.85	1.07	-0.02
23	perovskite_tec	2055	0	0	0.62	0.87	0.81	1.01	-0.07
24	perovskite_workfunction	3065	0	0	0.42	0.70	0.63	0.86	-0.07
24	phonon_freq	6325	0	0	0.93	0.95	0.73	0.97	-0.06
26	piezoelectric	4705	0	0	0.30	0.83	0.82	1.01	0.00
27	RPV_TTS	22675	0	0	0.58	0.83	0.72	0.98	-0.03
28	semiconductor_lvls	4480	0	0	0.41	0.79	0.74	0.92	-0.03
29	steel_yield	1560	0	0	0.62	0.88	0.73	0.92	-0.03
30	superconductivity	18756	0	0	0.48	0.88	0.8	1.00	-0.02
31	thermal_conductivity	13080	0	0	0.86	0.93	0.87	0.95	-0.12
32	thermalcond_aflow	24435	0	0	0.92	0.97	0.75	0.96	0.02
33	thermalexp_aflow	24430	0	0	0.87	0.97	0.89	1.17	-0.11

Table VI. Table V, followed.